Supplementary Material:
Modelling the flow of nocturnal bird migration with year-round European weather radar network.

Raphaël Nussbaumer, Lionel Benoit, Grégoire Mariethoz, Felix Liechti, Silke Bauer & Baptiste Schmid

1 Data Preprocessing

The processing of the raw weather radar data downloaded from the ENRAM repository (https://github.com/enram/data-repository) follows the general procedure described in Appendix A of Nussbaumer et al. (2019). Yet, we considerably improved the method of each steps, in particular the insect removal (1.3), filling the gaps (1.4) and vertical integration (1.5). The resulting dataset of the pre-processing is available at https://doi.org/10.5281/zenodo.3610184 Nussbaumer (2020).

1.1 Data selection

We downloaded all available data from 1 January 2018 to 1 January 2019 at the maximum resolution of 5 minutes. After a visual quality check, only the data from radars in France, Germany, Belgium and the Netherlands were retained, totalizing 37 radars (out of 107). We limit the analysis to night-time as defined by the local sunrise and sunset at each radar location. Because a manual cleaning (1.2) and an insect removal procedure (1.3) are employed, we used the bird reflectivity (η) output from vol2bird rather than bird density, and later convert it to bird density assuming a radar cross section of 11 cm^2 Dokter et al. (2011). Bird flight speed vector is computed on the East-West and North-South components based on the flight speed and direction.

1.2 Data cleaning

The vertical profile of bird density of each radar is manually cleaned using a MATLAB dedicated GUI program, as explained in points 2 and 3 in Appendix A of Nussbaumer et al. (2019). After manual cleaning, flight speed is only kept where bird density values are available, thus removing erroneous flight speed due to

rain and scattering. Gaps in flight speed are linearly interpolated when sufficient data is available around the gaps (i.e. 4 neighbours within 20minx800m). Finally, the full vertical profile of flight speed at a single time step is only kept if the altitude bins with measurements covers at least the equivalent of 50% of the total number of bird over this profile.

1.3 Insect removal

To remove insect contamination and residual rain with low reflectivity (e.g. snow shower), Dokter et al. (2011) recommend use a radial velocity standard deviation σ_{vvp} threshold of 2m/s prior to bird density estimation. However, this threshold tends to remove intense and strongly directed bird migration. Here, we developed a novel method based on distinguishing insects from birds based on both their different value of σ_{vvp} and airspeed. Indeed, birds' known air speed (8-10 m/s) is higher than insects' (around 2-3 m/s). Air speed was computed by subtracting the ground speed measured by the weather radar to the wind speed provided by the ERA reanalysis product at the same location and time (Copernicus Climate Change Service (C3S) (2017)). The proposed approach consists in fitting the joint pdf of airspeed and σ_{vvp} using a two-component Gaussian mixture model (one component represents birds, and the other insects, Figure 1). Using the whole 2018 dataset, the two fitted Gaussian components are

$$GM_{insect} = \mathcal{N}\left(\begin{bmatrix}2.6\\2.8\end{bmatrix}, \begin{bmatrix}1.8515 & 0.1716\\0.1716 & 1.1030\end{bmatrix}\right) \text{ and } GM_{bird} = \mathcal{N}\left(\begin{bmatrix}8.0\\4.1\end{bmatrix}, \begin{bmatrix}11.5019 & -1.1683\\-1.1683 & 0.9156\end{bmatrix}\right)$$

.

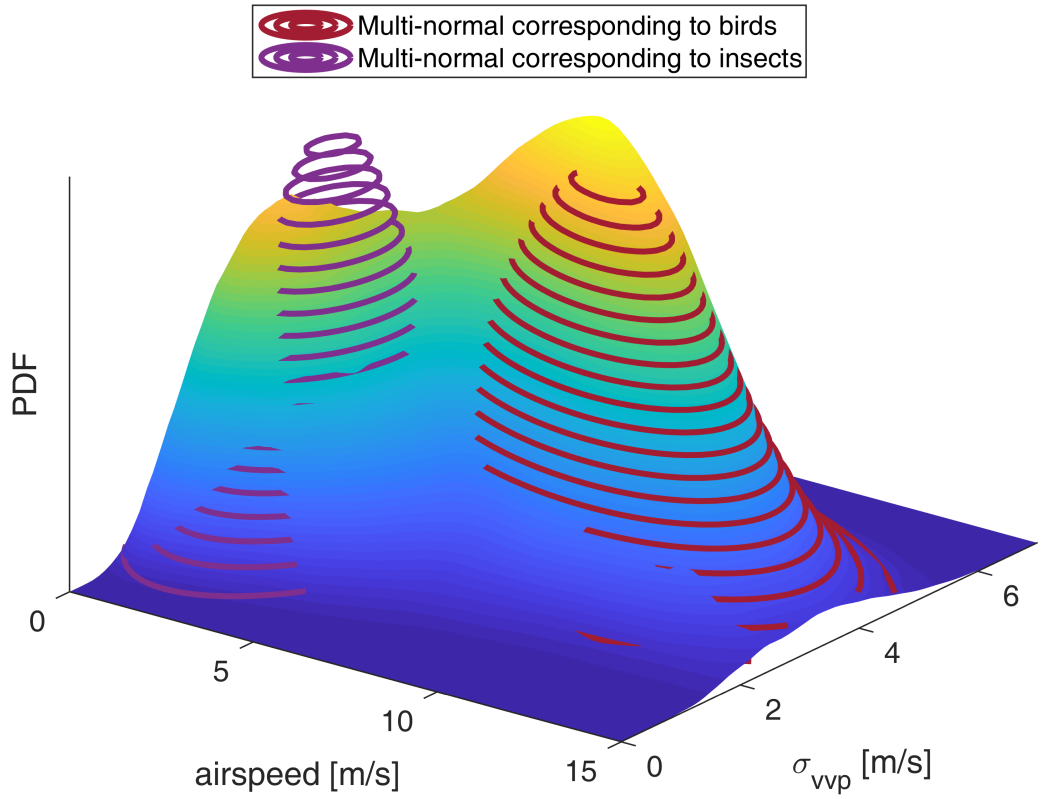

Figure 1. Joint probability distribution of airspeed and radial velocity standard deviation σ_{vvp}. The empirical function (surface in color scale) shows two peaks: the one on the right corresponds to birds and the one on the left to insects. The two multi-normal distribution fitted to the data are shown in contour lines.

The change in the proportion of birds and insects over the year is accounted for by fitting the amplitude of each Gaussian component for each month separately (Figure 2). By contrast, since we assume that insects and birds produce the same signature of airspeed and σ_{vvp}, the location and shape of each component are kept constant throughout the year.

The relative abundance of insects and birds not only varies over time but also over space (mainly latitude). In order to account for both the temporal and spatial variations, we fit the amplitude of the two Gaussians for each radar and each month. Rather than using an amplitude value for each component, we work with the proportion of components enforcing their sum to equal 1. Finally, the proportions fitted for each month are interpolated temporally with a shape-preserving piecewise cubic interpolation (pchip) function for each radar (Figure 3).

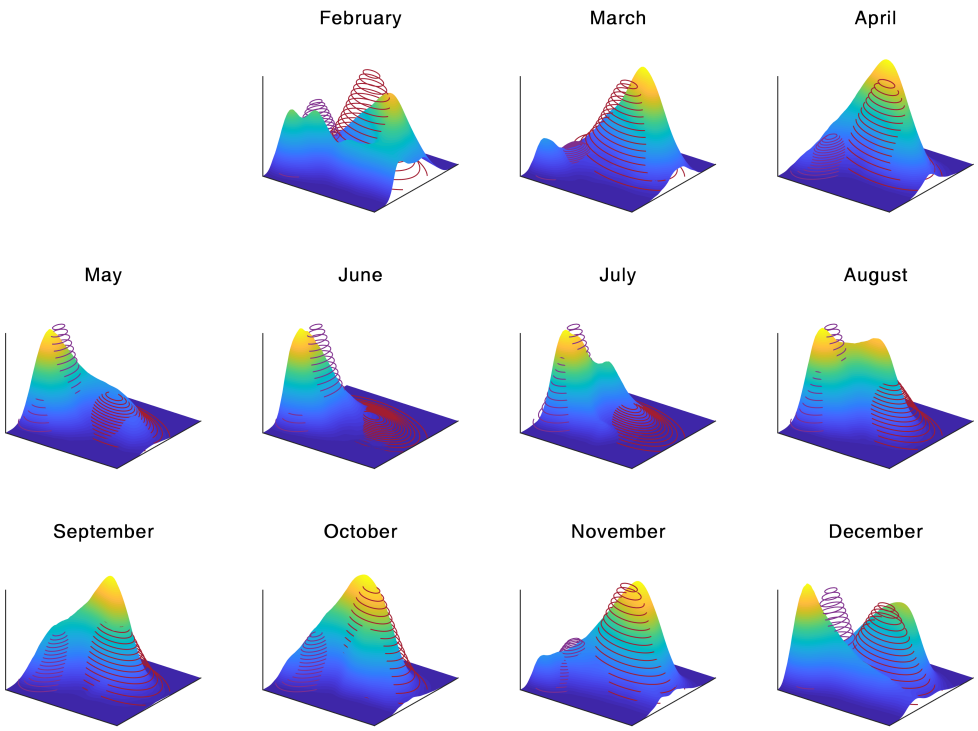

Figure 2. Joint pdf of airspeed and radial velocity standard deviation for the empirical (colour-scaled surface) and fitted Gaussian distributions of insects (red lines) and birds (purple lines). The axis unit and range are the same than in Figure 1. The parameters of location and scale of the two Gaussian components were determined based on all data combined (Figure 1). The amplitude (relative height) of the two distributions is adjusted for each month separately.
The overall quantity of birds decreases in the first half of the year and increases in the second. Insects start appearing in May and disappear from end of September. In winter, the insect-like signature recorded corresponds to snow, rain or remaining ground-scattering.

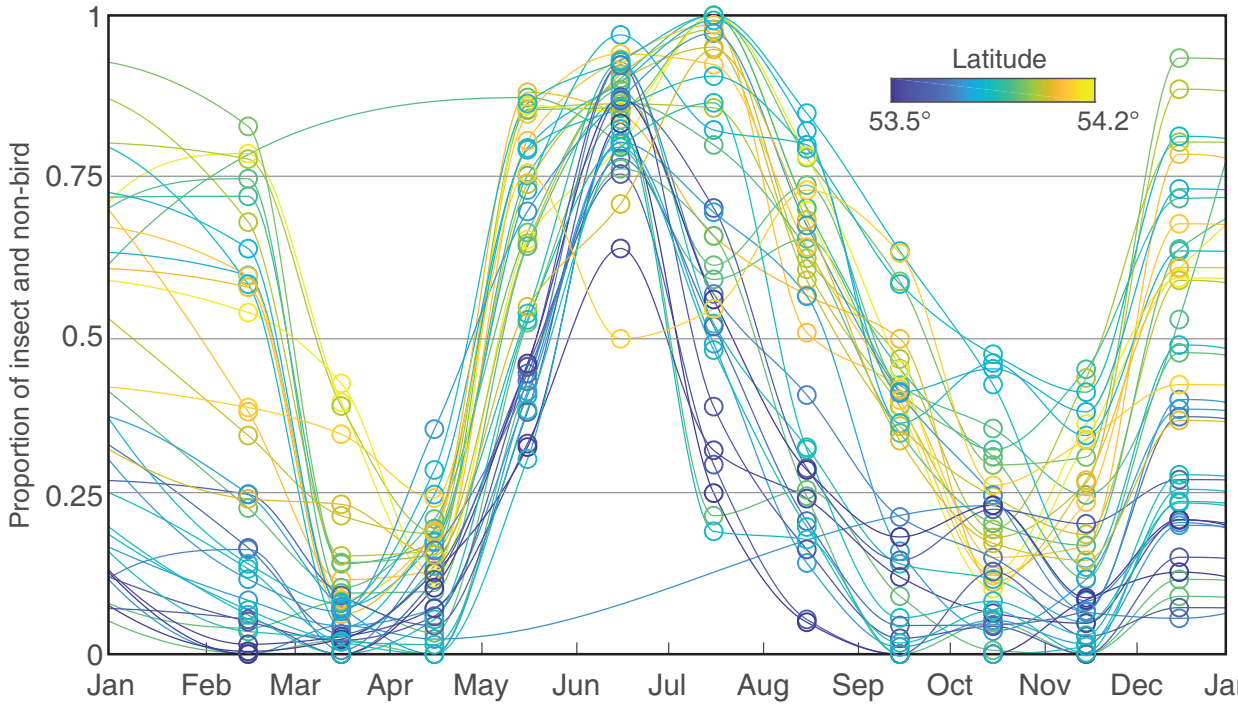

Figure 3. Proportion of non-bird signal varying along the year. Each line represents the interpolation at a given radar where the line colour corresponds to the latitude of the radar.

After quantifying the proportion of the non-bird signal, the bird density is corrected accordingly. Instead of using a threshold to define whether a certain measurement consists of bird or insect, we propose to use the proportion of insects estimated for each measurement to reduce accordingly the bird density of this measurement. Thus, we build the Gaussian pdfs of birds and insects based for each measurement based on the parameters of the Gaussians fitted in Figure 1 and with an amplitude according to the radar and day of year of the measurement according to Figure Figure 3 Using the air speed and σ_{vvp} of the measurement, we sample the two components to derive the probability of insects and birds. Finally, the proportion of insects is estimated by normalizing the probability of insects with the sums of probabilities of insects and birds. The bird density is finally corrected by multiplying the proportion of insects.

Bird's ground speed is also corrected from insect contamination. To this end, we increase the raw air speed amplitude $airspeed_{raw}$ proportionally to the proportion of insects estimated earlier. The coefficient of proportionality is taken as the difference of average air speed between the insect (2.4 m/s) and bird (8m/s) (Figure 1)]. The corrected airspeed becomes

$$airspeed_{corr} = airspeed_{raw} + (8 - 2.4) \times insect_{radar}.$$

Finally, the ground speed amplitude is determined by adding back the wind speed to the corrected air speed.

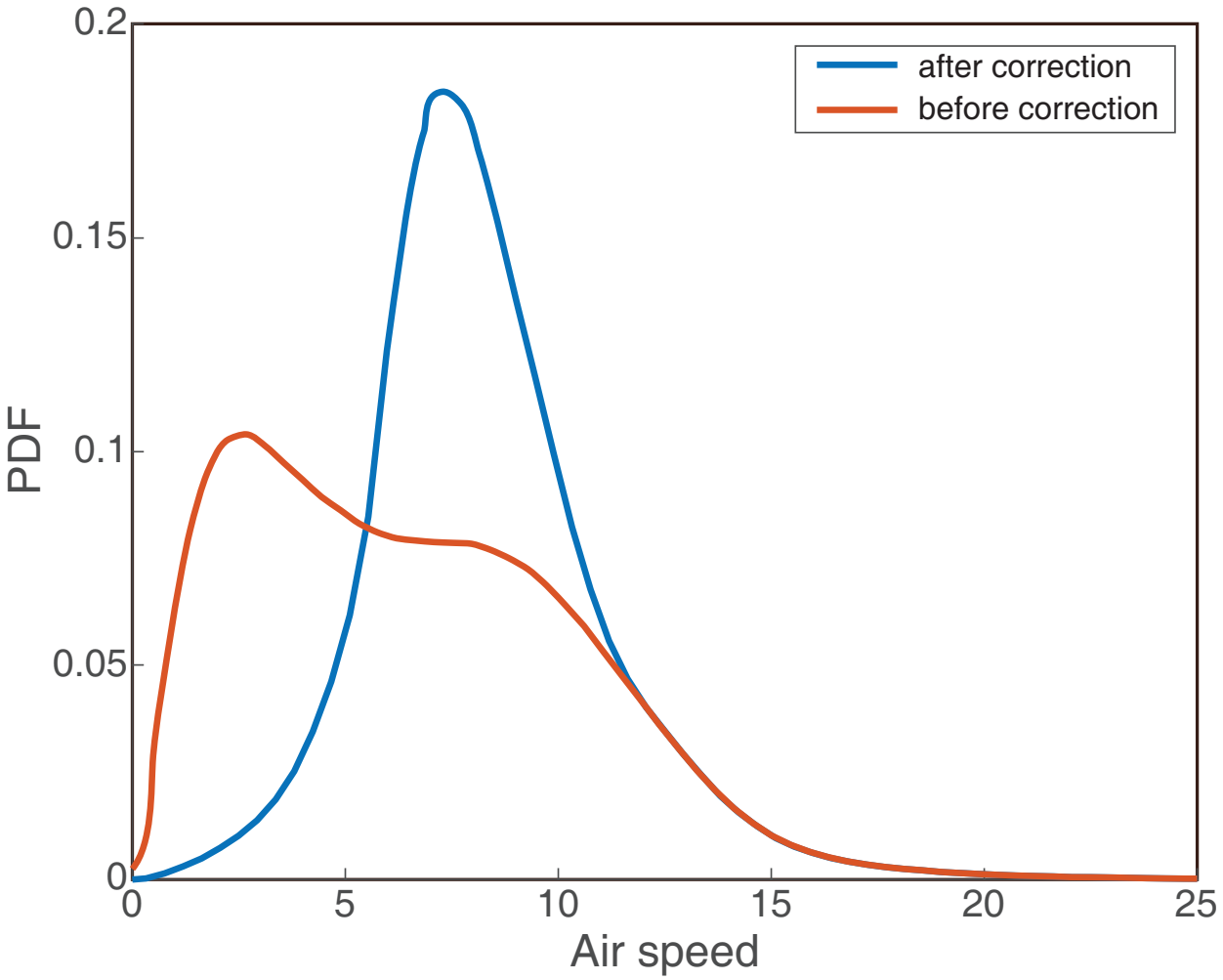

Figure 4. Air speed histogram of the full dataset before (red) and after (blue) correction. The histogram before correction shows two modes corresponding to insects (2.4m/s) and birds (8m/s). After correction, the insect mode is removed and the distribution is almost normally distributed.

1.4 Filling gaps in vertical bird density profiles

In this study, we improved the procedure of vertical bird density profile gap-filling proposed in Appendix A of cite(Nussbaumer2019).

Firstly, we remove vertical profile data isolated by at least 30 minutes and remove noise by interpolating log-linearly the grid cells with a value greater than twice the mean of its nine direct neighbours.

Secondly, instead of assuming a density of zero above the maximum height of measurement, we extrapolate the bird density up to 5000m asl. This is performed by assuming a density of 0 bird/km^3 at

5000m and using a vertical log linear interpolation.

Thirdly, we also developed a new methodology to interpolate bird density at the lowest altitudes. Indeed, due to ground scattering and the elevated position of weather radars, the bird density measured in the altitude bins lower or equal to radar elevation are often unknown or unreliable and yet they cover altitude were many bird might be migrating. In Nussbaumer et al. (2019), we copies the bird density value of the first non-contaminated bins all the way to the ground (i.e. equivalent to vertical nearest-neighbour interpolation). However, since bird density usually increases near the ground (see Figure 5) and thus represents a significant proportion of the total birds migrating, this process is prone to underestimate bird density.

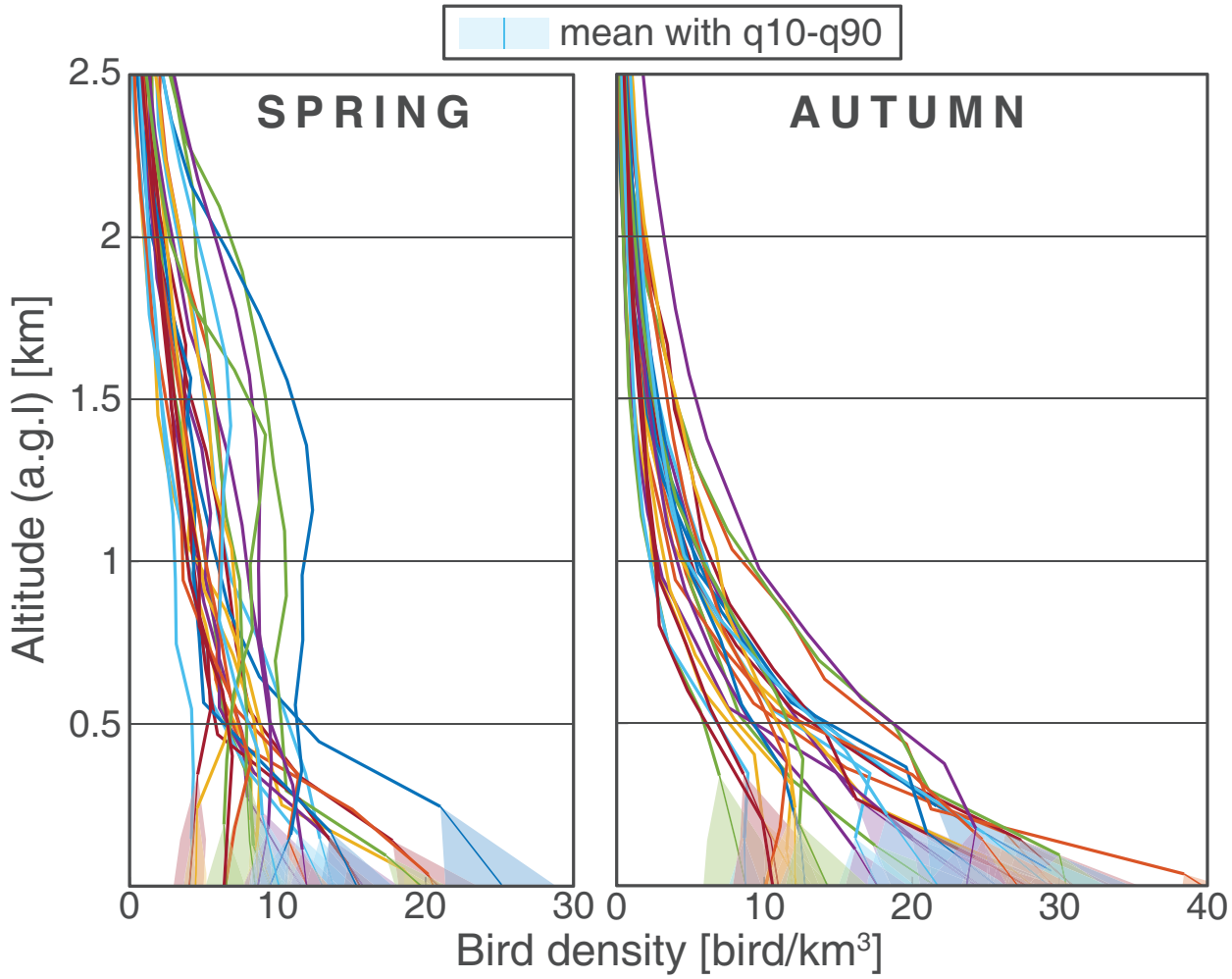

Figure 5. Average bird density vertical profile for multiple radars (colours) in spring (left) and autumn (right). Altitude is corrected with elevation of radar elevation. The radars are unable to measure bird density in the lower elevation, resulting in gaps in the dataset. These gaps are filled with a simulation method based on "image patching" (see below for details). The resulting simulations are shown with a thin line for the mean and as coloured area for the quantile 10 and 90.

To provide a more reliable estimate, we propose to resort to Multi-Point Statistic (MPS) to interpolate

low-altitude bins of bird density profiles. MPS is a simulation method based on patch matching (see Figure 6). For each value of bird density missing, the method searches for a similar neighbouring pattern (in time and space) amongst the other radars and pastes the central value of one of the most similar patches in the simulation. Since the bird density elevation profile changes over time (e.g. spring and autumn in Figure 5), the search of pattern is limited to the same period of the year. The computation of the MPS simulation is performed with Quantile Sampling (QS) Gravey and Mariethoz (2019), using the following parameters:

- Transformation: logarithm transformation prior to simulation and back transform post-simulation.
- Simulation path: starting with cells with higher altitude and going down.
- Training set: vertical profile of all other radars occurring during the same week as of the simulated night. Only the first 1000m above radar elevation are taken.
- Neighbourhood size: 15 with a uniform kernel of 49 x 7 cells (+/-2h, +/-500m).
- Best candidate: 1.5
- Realizations size: 30 realizations

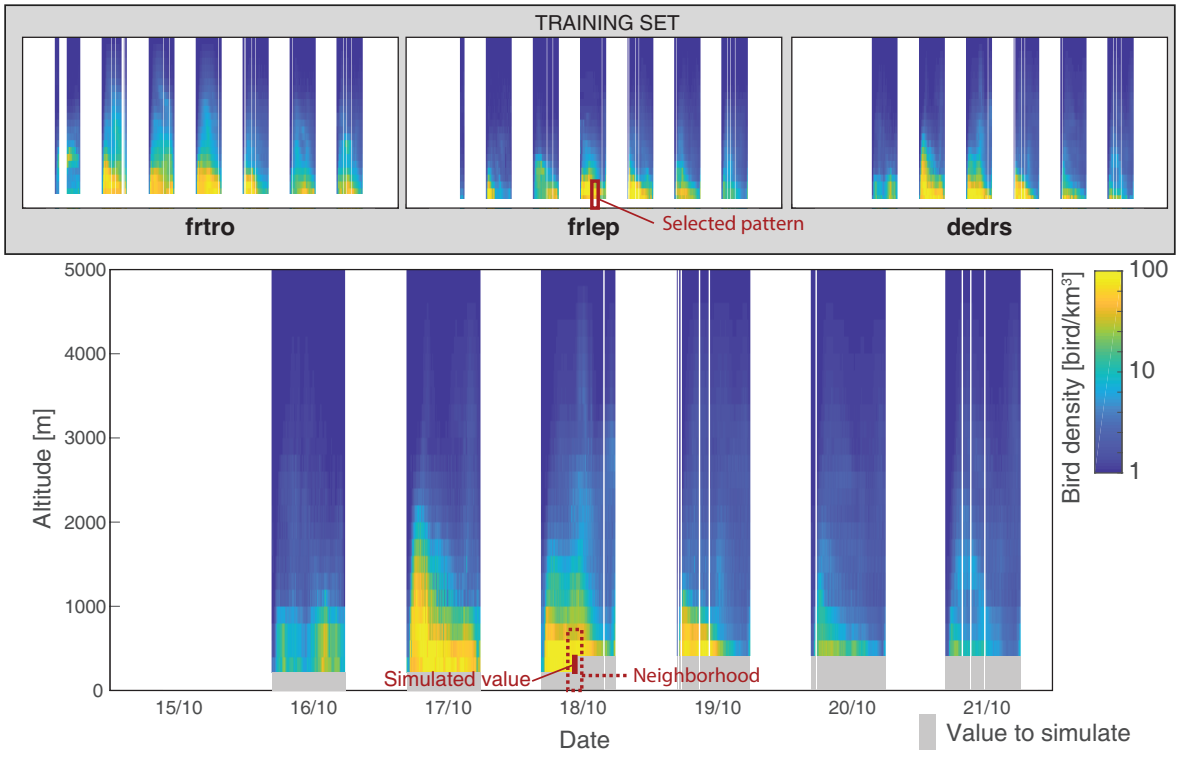

Figure 6. Illustration of the Multiple-Point Statistic (MPS) algorithm. The values to interpolate (in grey) are simulated one after the other. For each simulated value, a similar pattern as its neighbouring values is searched among the training set. The central value of the selected pattern in the training set become the simulated value.

1.5 Vertical Integration

After correcting the data for contamination of insect and filling gaps, the enhanced vertical profiles are integrated vertically, that is moving from volumetric density [bird/km^3] to surface density [bird/km^2]. The main novelty of this task is to account for local topography (Figure 7). Using the local flight direction of bird migration and a digital elevation model (Figure 7-1), we compute the elevation profile encountered by birds (perpendicular to flight direction) (Figure 7-2). Then, the volumetric bird density [bird/km^3] is weighted by the available air space in which birds can migrate (Figure 7-3). For computational reasons, this method is implemented by pre-computing the flight volume for each radar, a pre-defined set of flight direction and all altitude bins. In Figure 7, we express the flight volume as the difference between the new method and the

previous method, which only accounted for birds down to the radar altitude and without local topography.

Flight speed is simply integrated vertically by weighting the average with the bird density.

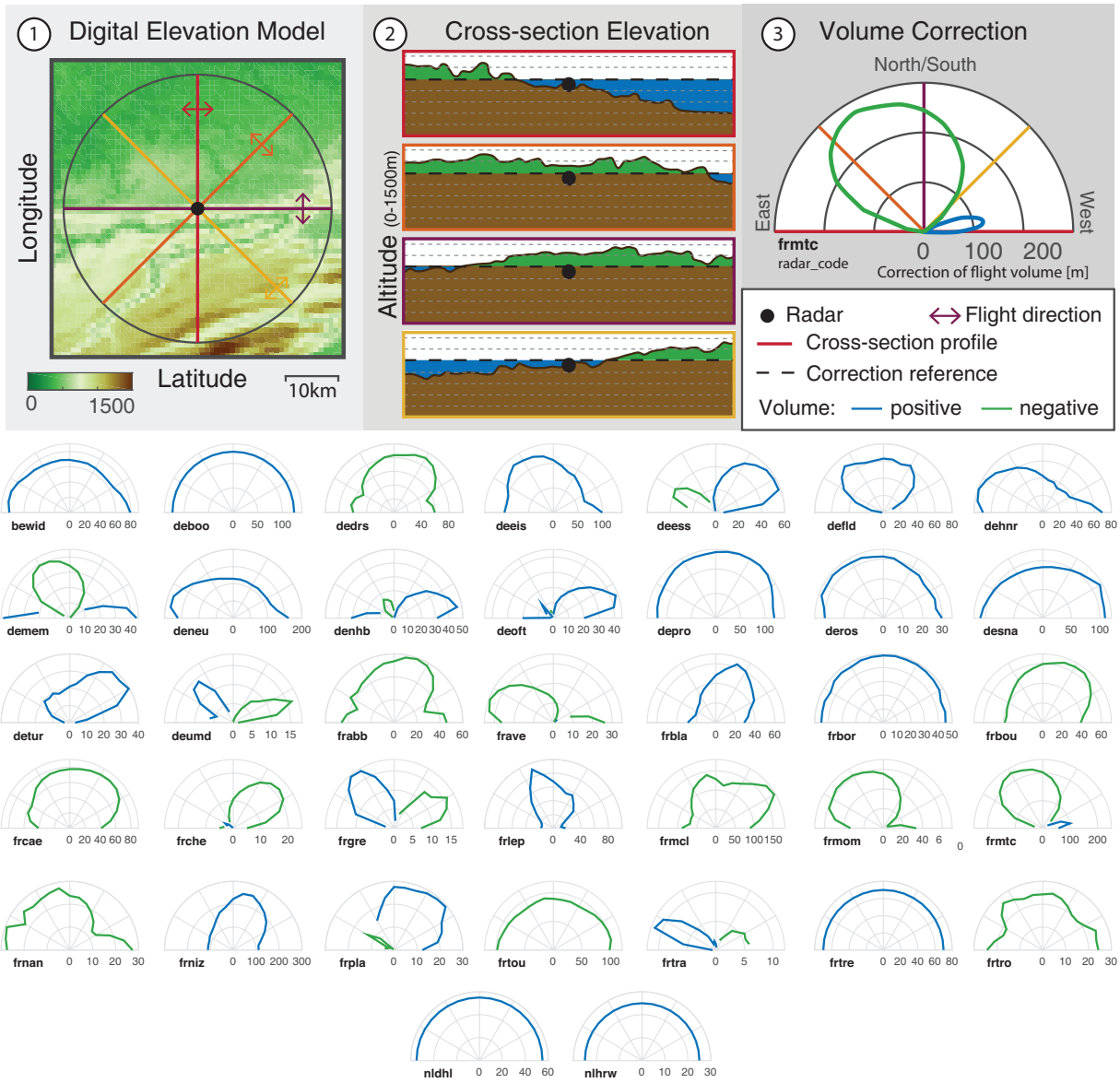

Figure 7. Difference of volume available for flight depending on the flight direction (0°is north and 90°is west.) Blue indicates a positive volume, and green a negative, compared to the previous method which used a flat topography located at radar altitude.

2 Adaptation of the interpolation method to year-round data

The interpolation of bird density follows the methodology presented in Nussbaumer et al. (2019) with the following changes to integrate year-round data:

- The power transformation is replaced by a quantile-quantile transformation of the kernel probability density fitted on the data.
- The inference and estimation are performed separately in four manually selected seasonal blocks (Figure 8).
- The areal bird density data produced by the pre-processing consists of 30 values simulated by the MPS simulation. The interpolation takes advantage of knowing this range of possible values by using the corresponding uncertainty to improve the trends of the geostatistical model (both temporal and spatial) with a generalized least square. In addition, a nugget effect is added to the kriging system to account for this uncertainty in the spatio-temporal covariance model.

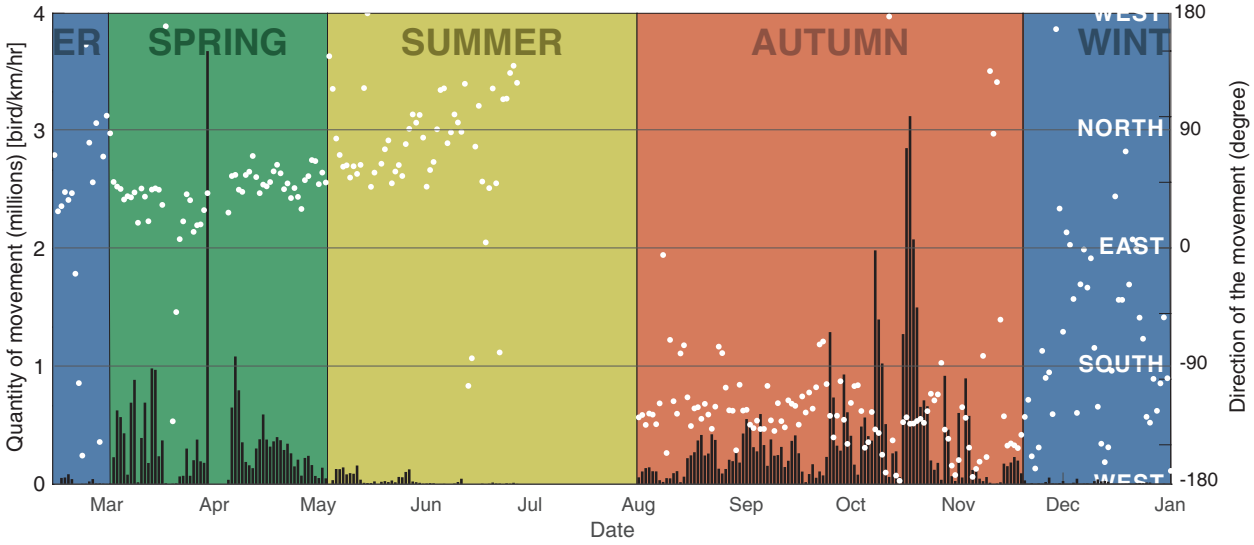

Figure 8. Summary of bird movement both in quantity and direction, based on the processed radar data. The average mean traffic rate (MTR) per night is shown as bar and the average weighted flight direction per night is illustrated with dots. This figure is used to separate the geostatistical model in four periods (winter, spring, summer and autumn), where the fit and estimation are done separately..

The interpolation of flight speed (both east-west and north-south components) is performed with a similar methodology than bird density with the following exceptions:

- No transformation is performed as the flight speed is close to normally distributed
- No trend was found in flight speed along the night (i.e. NNT). However, there was higher variability of flight speed at the beginning and end of the night, thus a variance trend was still performed.

References

Copernicus Climate Change Service (C3S). (2017). *ERA5: Fifth generation of ECMWF atmospheric reanalyses of the global climate.*

Dokter, A. M., Liechti, F., Stark, H., Delobbe, L., Tabary, P., & Holleman, I. (2011, jan). Bird migration flight altitudes studied by a network of operational weather radars. *Journal of The Royal Society Interface*, *8*(54), 30–43. doi:10.1098/rsif.2010.0116

Gravey, M., & Mariethoz, G. (2019). Quantile Sampling: a robust and simplified pixel-based multiple-point simulation approach. *Geoscientific Model Development Discussions*(November), 1–32. doi:10.5194/gmd-2019-211

Nussbaumer, R. (2020, jan). Vertical profiles time series of bird density and flight speed vector (01.01.2018-01.01.2019). doi:10.5281/zenodo.3610185

Nussbaumer, R., Benoit, L., Mariethoz, G., Liechti, F., Bauer, S., & Schmid, B. (2019, sep). A Geostatistical Approach to Estimate High Resolution Nocturnal Bird Migration Densities from a Weather Radar Network. *Remote Sensing*, *11*(19), 2233. doi:10.3390/rs11192233